

Proceeding Paper

Pregnancy Labor Prediction Using Magnetomyography Sensing and a Self-Sorting Cybernetic Model [†]

Ejay Nsugbe ^{1,*}, Oluwarotimi Williams Samuel ², Ibrahim Sanusi ³, Suresh Vishwakarma ⁴
and Dawn Adams ⁵

¹ Nsugbe Research Labs, Swindon SN1 3LG, UK

² Shenzhen Institute of Advanced Technology, Chinese Academy of Sciences, Shenzhen 518055, China; samuel@siat.ac.cn

³ Automatic Control and Systems Engineering, University of Sheffield, Sheffield S10 2TN, UK; enyone4ever@gmail.com

⁴ Utilities Engineering Unit, University of Trinidad and Tobago, 14-24 Keate Street, Port of Spain 100801, Trinidad and Tobago; sureshvishwakarma@hotmail.com

⁵ School of Computing, Ulster University, Newtownabbey BT37 0QB, UK; thatadamsone@yahoo.co.uk

* Correspondence: ennsugbe@yahoo.com

[†] Presented at the 8th International Electronic Conference on Sensors and Applications, 1–15 November 2021; Available online: <https://ecsa-8.sciforum.net>.

Abstract: To date, effective means of predicting pregnancy labor continues to lack. Magnetic field signals during uterine contraction have shown, in recent studies, to be a good source of information for predicting labor state with a greater accuracy compared with existing methods. The means of labor prediction methods from such signals appear to rely on a supervised learning post-processing framework whose calibration relies on an effective labelling of the training sample set. As a potential solution to this, using a reduced electrode channel from magnetomyography instrumentation, we propose a multi-stage self-sorting cybernetic model that is comprised of an ensemble of various post-processing methods, and is underpinned by an unsupervised learning framework that allows for an automated method towards learning from the trend in the data to infer labor state and imminency. Experimental results showed a comparable accuracy with those from a supervised learning method adopted in a prior study. Additionally, an architecture of how an intelligent cybernetic model can be used for labor prediction and cost saving benefits within a clinical setting is offered by this study.

Keywords: cybernetics; decision support; biosensors; unsupervised learning; electromagnetism; pregnancy; signal processing; obstetrics; artificial intelligence; intelligent systems



Citation: Nsugbe, E.; Samuel, O.W.; Sanusi, I.; Vishwakarma, S.; Adams, D. Pregnancy Labor Prediction Using Magnetomyography Sensing and a Self-Sorting Cybernetic Model. *Eng. Proc.* **2021**, *10*, 60. <https://doi.org/10.3390/ecsa-8-11312>

Academic Editor: Francisco Falcone

Published: 1 November 2021

Publisher's Note: MDPI stays neutral with regard to jurisdictional claims in published maps and institutional affiliations.



Copyright: © 2021 by the authors. Licensee MDPI, Basel, Switzerland. This article is an open access article distributed under the terms and conditions of the Creative Commons Attribution (CC BY) license (<https://creativecommons.org/licenses/by/4.0/>).

1. Introduction

The end of a pregnancy involves the expulsion of the fetus from the uterus, which commences with the thinning and dilation of the cervix, heightened contractions that aid in the ejection of the fetus, and finally the expulsion of the fetus and the placenta alongside further contractions to help reduce the loss of blood following the birth of a child [1]. An image showing the various stages associated with labor alongside the systematic changes that take place in the uterus can be seen in Figure 1. The ability to make a realistic prediction of when a woman is likely to go into labor allows for effective resource allocation to cater for the childbirth by a hospital, while also serving as a useful tool to determine if a probable preterm birth is likely to occur [2].

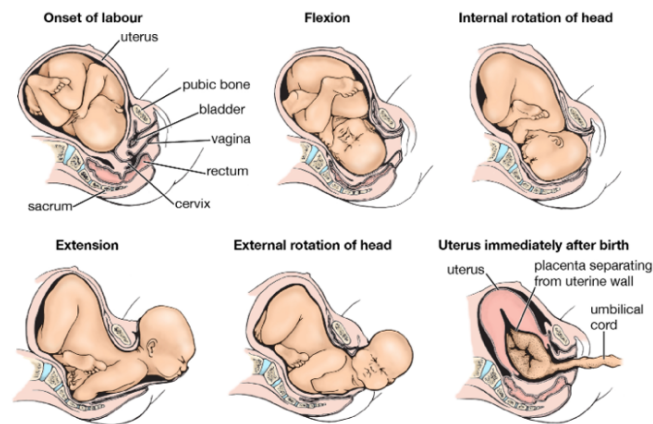


Figure 1. The core stages associated with labor and birth [3].

An example of a means of labor prediction includes the addition of 280 days to the woman's last menstrual period; this method can be viewed as a guess-based estimation which, in addition to its general inaccuracy, has been seen to be ineffective in developing countries where literacy skills continue to lack amongst members of the population [4].

During the third trimester of pregnancy, uterine contractions have been seen to occur, the recordings of which carry key information regarding the state of the fetus/pregnancy, with an appropriate set of signal processing algorithms for information decoding [5,6]. Previous studies have been conducted using acquired contraction signals to predict labor [1], in addition to predicting preterm, but the majority of these published studies have not considered the systemic subtleties as to how their designed model could fit in a clinical setting [1]. To address this apparent gap in the literature, this paper represents a study in an ongoing project around the design of decision support models, while taking a holistic view on the clinical aspects relating to model design [7].

Prior work done by the authors has looked at the application of a supervised learning framework, which employs the use of previously labelled data examples and this approach helps guarantee the selection of the optimal model parameters that allow for maximum recognition of the characteristics of interest in the data that it is being trained to identify [8]. In contrast, an unsupervised learning architecture allows for a fully automated self-learning approach towards the identification of trends and cluster separation, which correspond to discrete class labels for the classification problem [9]. In this paper, we propose a cybernetic model capable of 'self-sorting' and predicting labor and comprises of a four-stage identification process, namely: a metaheuristic signal decomposition phase, feature extraction, dimensionality reduction and an unsupervised learning/clustering phase [10].

The data used as part of this paper was acquired from non-invasive magnetomyography (MMG) signals from uterine contractions available on the Physionet database [11–13]. Due to the nature of the data, prediction classes are split between a labor imminency class of 0–48 h/48 h+ and comprise of data collected from Black, Caucasian and Hispanic ethnicities.

Specifically speaking, the contribution made in this manuscript is as below:

The application of a reduced channel MMG approach alongside a designed multi-stage cybernetic model for the prediction of pregnancy labor.

2. Materials and Methods

2.1. Magnetic Field

During anatomical uterine muscle contractions, electrophysiological ionic flow is said to be followed by a magnetic field, which is an orthogonal offset as per seminal work done by Faraday and Maxwell [14]. MMG sensors used for the acquisition of bio-magnetic signal manifestations are based off this principle and represent a non-invasive and safe means of recording bio-magnetic field signals which, in turn, carry a much stronger coupling to their primary sources due to the dynamic behavior of magnetic waves [14].

The governing principle behind electromagnetic fields from the uterine wall can be described as follows using quasistatic approximations of Maxwell’s formulas, with the assumption of a linear forward model, for a case of continuous current flow, Biot–Savart’s law can be used to convey the effect of magnetic fields from an electric source, which in turn can be used to estimate the magnetic field, as shown in Equation (1) [14,15]:

$$B(r) = \frac{\mu_0}{4\pi} \int \frac{J(r') \times l}{l^3} dv' \tag{1}$$

B represents Biot–Savart’s law, $l = r - r'$ is a vector emanating from the source r' to the point of observation r to an observed point whose magnitude is $= ||l||_2$, μ_0 is the permeability of free space, while $J(r')$ is the current density from the source.

Expressing the ratio of l/l^3 as $-\nabla'(\frac{1}{l}) = \nabla'(\frac{l}{l^3})$, we yield (1) as follows:

$$B(r) = \frac{\mu_0}{4\pi} \int J(r') \times \nabla' \frac{l}{l^3} dv' \tag{2}$$

∇ is the del operator that signifies the derivative of a function in vector calculus, ∇' is the derivative of the del operator.

Assuming rapid current density dissipation (2) can be rewritten as:

$$B(r) = \frac{\mu_0}{4\pi} \int \frac{\nabla' \times J(r')}{l} dv' \tag{3}$$

Due to superposition of electric fields from both volume and primary current, a linear expression can thus be deduced between the magnetic field B and the accompanying source current density J^p , which ultimately permits for the calculation of the potential given V as shown in (4) [14,15]:

$$B(r) = \frac{\mu_0}{4\pi} \int \left(J^p(r') + V(r') \nabla' \sigma(r') \right) \times \frac{l}{l^3} dv' \tag{4}$$

σ is the macroscopic conductivity of the volume conductor.

2.2. MMG Dataset

The source of the MMG data used as part of this paper is from the Physionet database, which holds the MMG signals recorded using the 151-channel SQUID Array for Reproductive Assessment (SARA), which is a passive operational device for the acquisition of magnetic field signals [11–13]. Magnetic shielding was employed to prevent external sources of interference and the study received ethical approval from the University of Arkansas for Medical Sciences Institutional Review Board, and an informed consent was obtained from participants prior to the data collection process [11–13].

The MMG data consisted of a total of 25 patients, all of whom were in their third trimester of pregnancy, the acquisition rate for data recording was at 250Hz, which was down-sampled to 32Hz [11–13]. Since the data was acquired at a variable rate of 10–20 min between different subjects, only the first 10 min from each subject was used for the signal processing work in this paper, as a means of standardization [11–13].

It should be noted that, due to errors encountered while downloading the dataset, the data used were from a total of 22 patients, and 5 MMG channels were used as part of the signal processing exercise.

An image showing the concept of the acquisition of an MMG field signal from a pregnant patient can be seen in Figure 2.

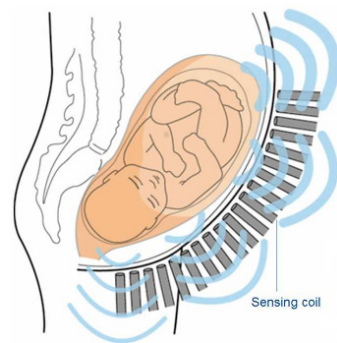


Figure 2. Acquisition of uterine contraction signals from a pregnant patient [15].

2.3. Cybernetic Model

In the interest of parsimony and promotion of affordability of the MMG instrumentation, only an arbitrarily selected first five of the total electrode channels from the MMG were used for the model build work in this paper, building on the results from previous work [16].

2.3.1. Signal Decomposition

During anatomical contraction, there exists a large number of motor neurons simultaneously, which leads to a superposition of the output waves acquired with the associated physiological instrumentation, the decomposition of a signal has been seen to enhance the overall signal quality, and thus classification accuracy [17].

The signal decomposition method used as part of the cybernetic model is the bespoke linear series decomposition learner (LSDL), which uses a series of linear thresholds as the basis function for the deconvolution of the signal [18]. It was originally designed for source separation of mixture signals, and has recently been extended towards deconvolution of brain waves and neuromuscular signals in the area of rehabilitation medicine and upper-limb prosthesis control [17,18]. Over a number of case studies, results have shown that its performance is superior to that of the wavelet decomposition in terms of performance and computational complexity [17,19,20].

The LSDL is a metaheuristic algorithm that uses a series of linear thresholds of a given magnitude, alongside a peak detection method, to iteratively deconvolve a stochastic time-series into a set of sub-time series [17–20]. From this, all sub-time series are assessed via a performance index to obtain an optimal decomposition region that can be parameterized by its spatial parameters. This represents a region within the stochastic time-series from the same source, and maximizes prediction power and minimizes uncertainty. The optimal decomposition region is denoted as X_{opt} , and represents the region from the time-series that should be used for further analysis in order to maximize prediction and modelling accuracy, assuming the recording instrumentation and the source remains unchanged. Key steps associated with the LSDL decomposition can be seen in Refs. [17,18].

2.3.2. Feature Extraction

A select list of features are to be extracted from the signal at this stage, and can be seen as follows: MP, WL, slope sign change (SSC), root mean squared (RMS), sample entropy (SampEN), cepstrum (Ceps), maximum fractal length (MFL), median frequency of power spectrum (MF), simple squared integral (SSI) and variance (VAR) [16,21]. The list of candidate features to be extracted comprises a smaller set of features when compared to related studies that have worked with this dataset—this is due to the advantages offered by the LSDL—i.e., an optimal decomposition of the signal that allows for a more parsimonious signal modelling [16]. The threshold value used for the calculation of the SSC was $1 \mu\text{v}$, while the SampEN was computed using m as 2 and r as 0.2.

It should be noted that, for the results described as part of Section 3, the SMOTE artificial sample generator algorithm was used for the increment of training examples and for class balancing.

2.3.3. Dimensionality Reduction

The concept of dimensionality reduction refers to methods that are used to compress and trim down what ordinarily would be a high dimension vector, thus removing redundancies from the data and ultimately allowing for quicker post-processing of the reduced dimensional vector, after reduction [22]. The principal component analysis (PCA) is a linear dimensionality reduction method that has been seen in previous studies to be optimal for a lower dimensional embedding of feature vectors from uterine contraction signals [22]. The mathematical flow and framework behind the PCA method can be seen in [23]. In this step, the first two PCs were selected, which accounted for 95%+ of the variability of the data, thus effectively compressing the data that comprises 10 columns to two.

2.3.4. Unsupervised Learning and Labor Prediction

In this final stage, the two PCs are projected into feature space where clustering and data classes are formed to represent the two possible labor states.

The Gaussian mixture model (GMM) represents a probabilistic unsupervised learning model that was used for the clustering exercise in this paper [24]. As the classification problem at hand involved a two-cluster assignment, an a priori value of 2 would need to be set as a default during this stage. The GMM's architecture can be described as a parametrized mixture that can be described by its mean and associated co-variances. The iterative learning procedure of the GMM is based on the expectation-maximization (E-M), which works with the maximum likelihood estimation sequence [23,24].

In this work, the GMM was used with the hard clustering option where each data point is assigned a single cluster only. A flow sequence representation of the cybernetic labor prediction model showing the various stages, can be seen in Figure 3.

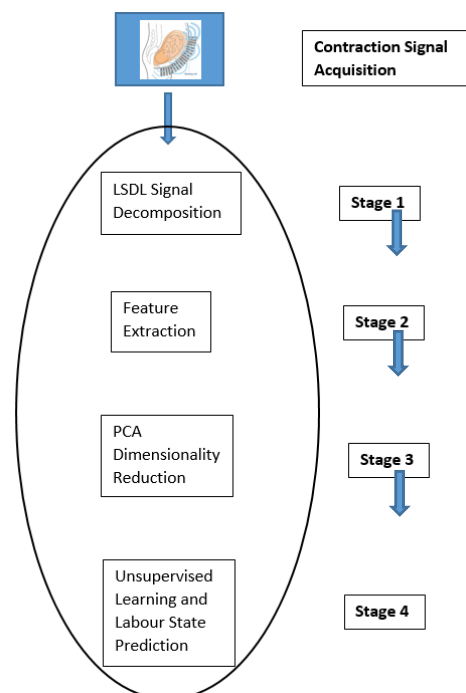


Figure 3. Flow diagram showing the different stages of the cybernetic prediction model.

3. Results and Conclusions

The optimal decomposition level of the signal from the LSDL was seen to be from the third iteration of the upper-threshold region. The performance of the cybernetic model was assessed using hold-out data, which comprised of an unseen 20% of the whole dataset, which was utilized as the test set. The model converged within 30 iterations and had a mixture proportion of 0.486 and 0.514, where the mixture proportion reflects an acceptable, bias for data points to be clustered in cluster two. The results of the initial cluster assignment and model training provided an accuracy of 84.9%, while the hold-out result produced an accuracy of 85.4%, thereby showing good capability of sorting through the various labor states.

A principal component analysis (PCA) visualization of the two labor state classes with the true classes plotted can be in Figure 4, where it can be seen in contrast that the extent to which labor states can be distinguished using this cybernetic model hinges on the inclusion of the LSDL to help reduce the uncertainty from the signal, which can allow for a more effective cluster assignment process.

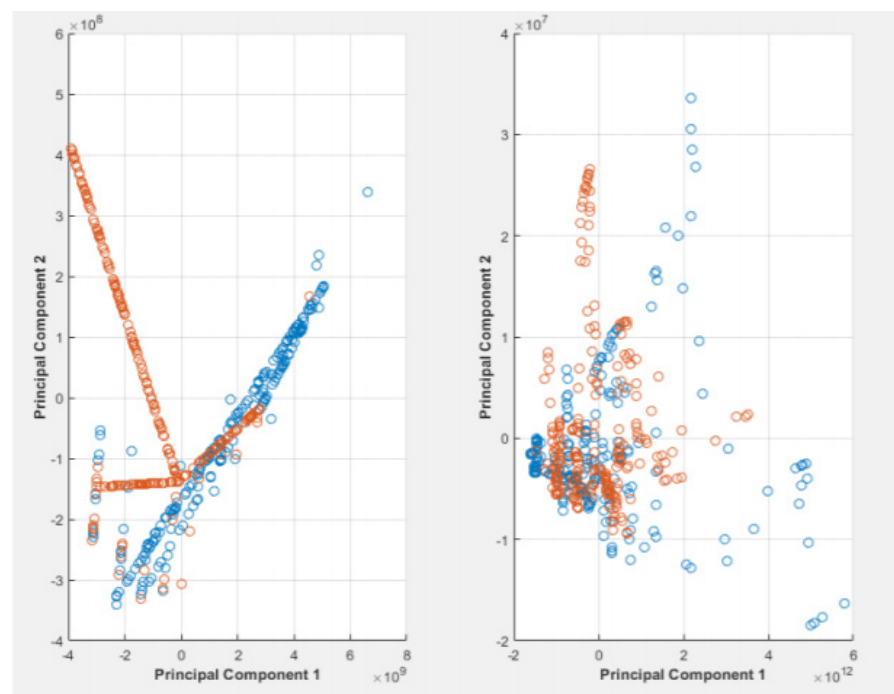


Figure 4. PCA plot showing cluster separation with the LSDL (**left**) and without pre-processing with the LSDL (**right**), where blue cluster-class 1/0–48 h, and red cluster-class 2/48 h+.

Compared to previous work, which applied the supervised learning framework to achieve accuracies of about 90%, although the results are slightly lower, the proposed cybernetic framework allows for a greater automated decision support framework that is self-sorting, thus implicitly providing a framework with cost saving benefits [16]. Additionally, the method proposed in this study may find applications in the domain of intelligent clinical decision support system targeted towards chronic disease diagnoses [25]. With a view to enhancing the classification prowess of the cybernetic model, a fifth stage could be included where the automated labelling of the data is conducted in the prior stage using the GMM, and thus fed into a more powerful supervised learning model for the final classification decision, although this inclusion will increase the overall model complexity associated with the classification process.

Author Contributions: E.N. conceptualised the work, processed the data and wrote the draft of the manuscript; I.S., O.W.S., S.V. and D.A. provided feedback and technical input on the manuscript drafts. All authors have read and agreed to the published version of the manuscript.

Funding: This research received no external funding.

Institutional Review Board Statement: Not applicable.

Informed Consent Statement: Not applicable.

Data Availability Statement: Data is available via a cited database in the manuscript.

Acknowledgments: The authors would like to thank Brian Kerr for proofreading the manuscript.

Conflicts of Interest: The authors declare no conflict of interest.

References

- Offiah, I.; Odonoghue, K.; Kenny, L. Clinical Risk Factors for Preterm Birth. In *Preterm Birth—Mother and Child*; Morrison, J., Ed.; InTech: Vienna, Austria, 2012; ISBN 978-953-307-828-1.
- Oskovi Kaplan, Z.A.; Ozgu-Erdinc, A.S. Prediction of Preterm Birth: Maternal Characteristics, Ultrasound Markers, and Biomarkers: An Updated Overview. *J. Pregnancy* **2018**, *2018*, 8367571. [[CrossRef](#)] [[PubMed](#)]
- Birth—Fetal Presentation and Passage through the Birth Canal. Available online: <https://www.britannica.com/science/birth> (accessed on 1 May 2021).
- Alberola-Rubio, J.; Garcia-Casado, J.; Prats-Boluda, G.; Ye-Lin, Y.; Desantes, D.; Valero, J.; Perales, A. Prediction of Labor Onset Type: Spontaneous vs. Induced; Role of Electrohysterography? *Comput. Methods Programs Biomed.* **2017**, *144*, 127–133. [[CrossRef](#)] [[PubMed](#)]
- Moslem, B.; Hassan, M.; Khalil, M.; Marque, C.; Diab, M.O. Monitoring the Progress of Pregnancy and Detecting Labor Using Uterine Electromyography. In Proceedings of the 2009 International Symposium on Bioelectronics & Bioinformatics, Melbourne, Australia, 9–11 December 2009.
- Nsugbe, E.; Samuel, O.W.; Sanusi, I.; Asogbon, M.G.; Li, G. A Study on Preterm Predictions Using Physiological Signals, Medical Health Record Information and Low Dimensional Embedding Methods. *IET Cyber-Syst. Robot.* **2021**, *3*, 228–244. [[CrossRef](#)]
- Nsugbe, E.; Obajemu, O.; Samuel, O.W.; Sanusi, I. Enhancing Care Strategies for Preterm Pregnancies by Using a Prediction Machine to Aid Clinical Care Decisions. *Mach. Learn. Appl.* **2021**, *6*, 100110. [[CrossRef](#)]
- Nsugbe, E.; Obajemu, O.; Samuel, O.W.; Sanusi, I. Application of non-invasive magnetomyography in labor imminency prediction for term and preterm pregnancies and ethnicity specific labor imminency prediction. *Mach. Learn. Appl.* **2021**, *5*, 100066.
- Soni, D. Supervised vs. Unsupervised Learning. Available online: <https://towardsdatascience.com/supervised-vs-unsupervised-learning-14f68e32ea8d> (accessed on 1 May 2021).
- Wiener, N. *Cybernetics: Or, Control and Communication in the Animal and the Machine*, 2nd ed.; The MIT Press: Cambridge, MA, USA, 2019; ISBN 978-0-262-53784-1.
- Escalona-Vargas, D.; Govindan, R.B.; Furdea, A.; Murphy, P.; Lowery, C.L.; Eswaran, H. MMG Database. *PhysioNet*, 4 March 2016.
- Escalona-Vargas, D.; Govindan, R.B.; Furdea, A.; Murphy, P.; Lowery, C.L.; Eswaran, H. Characterizing the Propagation of Uterine Electrophysiological Signals Recorded with a Multi-Sensor Abdominal Array in Term Pregnancies. *PLoS ONE* **2015**, *10*, e0140894. [[CrossRef](#)] [[PubMed](#)]
- Goldberger, A.L.; Amaral, L.A.; Glass, L.; Hausdorff, J.M.; Ivanov, P.C.; Mark, R.G.; Mietus, J.E.; Moody, G.B.; Peng, C.K.; Stanley, H.E. PhysioBank, PhysioToolkit, and PhysioNet: Components of a New Research Resource for Complex Physiologic Signals. *Circulation* **2000**, *101*, E215–E220. [[CrossRef](#)] [[PubMed](#)]
- La Rosa, P.S.; Eswaran, H.; Preissl, H.; Nehorai, A. Multiscale Forward Electromagnetic Model of Uterine Contractions during Pregnancy. *BMC Med. Phys.* **2012**, *12*, 4. [[CrossRef](#)] [[PubMed](#)]
- Zhang, M.; La Rosa, P.S.; Eswaran, H.; Nehorai, A. Estimating Uterine Source Current during Contractions Using Magnetomyography Measurements. *PLoS ONE* **2018**, *13*, e0202184. [[CrossRef](#)] [[PubMed](#)]
- Nsugbe, E.; Sanusi, I. Towards an Affordable Magnetomyography Instrumentation and Low Model Complexity Approach for Labour Imminency Prediction Using a Novel Multiresolution Analysis. *Appl. AI Lett.* **2021**. [[CrossRef](#)]
- Nsugbe, E.; Samuel, O.W.; Asogbon, M.G.; Li, G. Contrast of multi-resolution analysis approach to transhumeral phantom motion decoding. *CAAI Trans. Intell. Technol.* **2021**, *6*, 360–375. [[CrossRef](#)]
- Nsugbe, E.; Ruiz-Carcel, C.; Starr, A.; Jennions, I. Estimation of Fine and Oversize Particle Ratio in a Heterogeneous Compound with Acoustic Emissions. *Sensors* **2018**, *18*, 851. [[CrossRef](#)] [[PubMed](#)]
- Nsugbe, E.; Starr, A.; Ruiz Carcel, C. Monitoring the Particle Size Distribution of a Powder Mixing Process with Acoustic Emissions: A Review. *Eng. Technol. Ref.* **2012**, 1–12. [[CrossRef](#)]
- Nsugbe, E.; Starr, A.; Foote, P.; Ruiz-Carcel, C.; Jennions, I. Size Differentiation of a Continuous Stream of Particles Using Acoustic Emissions. *IOP Conf. Ser. Mater. Sci. Eng.* **2016**, *161*, 012090. [[CrossRef](#)]
- Phinyomark, A.; Limsakul, C.; Phukpattaranont, P. Application of Wavelet Analysis in EMG Feature Extraction for Pattern Classification. *Meas. Sci. Rev.* **2011**, *11*, 45. [[CrossRef](#)]
- Jolliffe, I.T.; Cadima, J. Principal Component Analysis: A Review and Recent Developments. *Philos. Trans. R. Soc. A* **2016**, *374*, 20150202. [[CrossRef](#)] [[PubMed](#)]
- Nsugbe, E.; Samuel, O.W.; Asogbon, M.G.; Li, G. A Self-Learning and Adaptive Control Scheme for Phantom Prosthesis Control Using Combined Neuromuscular and Brain-Wave Bio-Signals. *Eng. Proc.* **2020**, *2*, 59. [[CrossRef](#)]

-
24. Carrasco, O.C. Gaussian Mixture Models Explained. Available online: <https://towardsdatascience.com/gaussian-mixture-models-explained-6986aaf5a95> (accessed on 4 May 2021).
 25. Samuel, O.W.; Asogbon, G.M.; Sangaiah, A.K.; Fang, P.; Li, G. An Integrated Decision Support System Based on ANN and Fuzzy_AHP for Heart Failure Risk Prediction. *Expert Syst. Appl.* **2017**, *68*, 163–172. [[CrossRef](#)]